

Performance characteristics of cw InGaN multiple-quantum-well laser diodes

Michael Kneissl*, William S. Wong, Chris. G. Van de Walle, John E. Northrup, David W. Treat, Mark Teepe, Naoko Miyashita, Peter Kiesel, Noble M. Johnson

Electronic Materials Laboratory, XEROX Palo Alto Research Center,
3333 Coyote Hill Road, Palo Alto, CA 94304, U.S.A.

ABSTRACT

The performance characteristics are reported for continuous-wave (cw) InGaN multiple-quantum-well laser diodes grown on epitaxially laterally overgrown GaN on sapphire substrates by metalorganic chemical vapor deposition. Room-temperature cw threshold currents as low as 41mA with operating voltages of 6.0V were obtained. The emission wavelength was near 400 nm with output powers greater than 20 mW per facet. Under cw conditions laser oscillation was observed up to 90°C. A significant reduction in thermal resistance was observed for laser diodes transferred from sapphire onto Cu substrates by excimer laser lift-off, resulting in increased cw output power of more than 100mW.

INTRODUCTION

Since the first demonstration of an InGaN multiple-quantum-well (MQW) laser diode in 1995 [1] enormous progress has been made with the currently most advanced devices operating under cw conditions and lifetimes greater than 15000 hours [2,3,4]. The commercialization of violet laser diodes was recently announced [5], targeting a wide range of applications particularly high-density optical data storage and printing. In order to improve the performance and lifetime of group III-nitride laser diodes, the reduction of the dislocation density in the material has shown to be a pivotal step. As Nakamura and co-workers have demonstrated by employing an epitaxial lateral overgrowth technique [2,3], the dislocation density in GaN films grown on sapphire can be reduced from $\sim 10^{10} \text{cm}^{-2}$ to $\sim 10^6 \text{cm}^{-2}$, thus greatly enhance the performance of laser diodes. In the meantime a number of other groups have realized room-temperature cw operation of InGaAlN laser diodes [6,7,8,9] using a variety of techniques to reduce the dislocation density in GaN materials [10,11,12]. In this paper we report on the performance characteristics of InGaN MQW laser diodes grown on low-dislocation density epitaxially laterally overgrown (ELOG) GaN on sapphire substrates and compare these to results obtained on laser diodes directly grown on sapphire substrates. We also discuss the effect of the substrate thickness and material on the thermal impedance of laser diodes and demonstrate improved thermal resistance for laser diodes transferred from the sapphire substrate onto Cu using excimer laser-lift-off.

* Electronic mail: kneissl@parc.xerox.com

EXPERIMENTAL RESULTS

A schematic of a laser diode structure is shown in Fig. 1. The InGaAlN heterostructure was grown by metalorganic chemical vapor deposition (MOCVD) on (0001) c-face sapphire substrates. First a 4 μm thick GaN film was deposited on the sapphire substrate followed by a 100 nm thick layer of silicon dioxide (SiO_2). The SiO_2 film was subsequently patterned to form an 8 μm wide stripe pattern with a period of 11 μm parallel to the $\langle 10\text{-}10 \rangle$ direction of the GaN. MOCVD growth was then resumed and a 15 μm -thick, Si-doped GaN layer deposited on the patterned substrate. The growth was

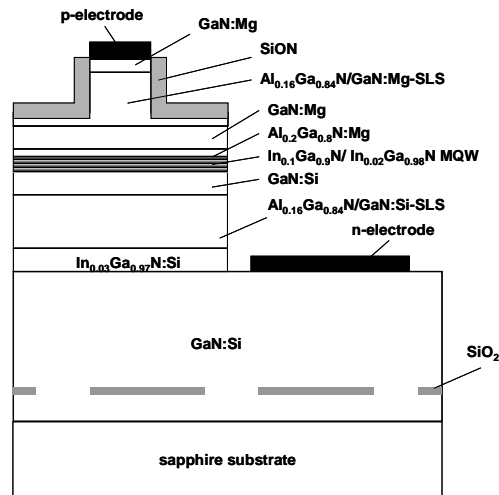


Figure 1: Schematic of a ridge-waveguide laser structure on sapphire substrate.

completed with a laser diode heterostructure as follows: a 0.1- μm -thick Si-doped InGaAlN defect reducing layer, a 1- μm -thick Si-doped AlGaIn/GaN strained-layer-superlattice cladding layer, an active region comprised of three 35 \AA thick InGaAlN quantum wells sandwiched between 0.1- μm -thick GaN waveguiding layers, a 20-nm Mg-doped AlGaIn tunnel barrier layer grown on top of the MQW, a 0.5- μm -thick Mg-doped AlGaIn/GaN strained-layer-superlattice cladding layer, and finally a 50 nm-thick Mg-doped GaN contact layer. After MOCVD growth, a ridge waveguide structure was formed by etching into the upper cladding layer with chemical assisted ion beam etching (CAIBE). Subsequently mesas and mirrors for the edge-emitting laser diodes were fabricated also by using CAIBE. Then metal contacts were deposited on the exposed n-type GaN layer for the lateral electrical connection and on top of the p-type GaN layer. In order to reduce the mirror loss, a high-reflective dielectric coating ($R \sim 90\%$) was deposited on the backside mirror facet. For improved thermal management the sapphire substrate was thinned to about 200 μm and the laser device was mounted p-side up onto a copper heat sink.

An important step to enhance the performance of the laser diodes was to reduce the dislocation density in the InGaAlN films. In order to determine and provide fast

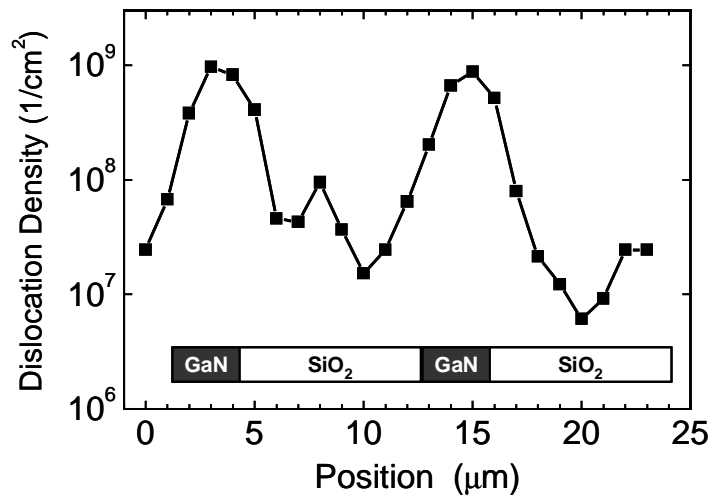


Figure 2: Measured dislocation density along the $\langle 10\text{-}10 \rangle$ direction of an ELOG substrate.

feedback of the density of threading dislocations in the ELOG films we used a selective photo-enhanced wet-chemical etching technique. The samples were patterned with Ti/Au stripes to serve as anodes and then etched in an electrochemical cell using a 0.008 M KOH solution under illumination with an Hg arc lamp. By selectively etching away the material around the threading dislocations, edge and mixed dislocations are revealed as whiskers on the surface of the etched ELOG substrate. Details of this etching technique can be found in Refs. 13 and 14. A count of the dislocation density measured along the $\langle 10\text{-}10 \rangle$ direction is shown in Fig. 2. As expected a relatively high dislocation density in the order of $\sim 10^9 \text{ cm}^{-2}$ was found around the GaN seed region. A significantly reduced dislocation density in the order of $\sim 10^7 \text{ cm}^{-2}$ was found around the ELOG wing regions. Towards the middle of the SiO_2 stripes were the growth fronts from the left and right side of the ELOG wing regions coalesce the dislocation density increases again. These results were in good agreement with dislocation densities determined by plan-view transmission electron microscopy (PTM) with $< 5 \times 10^7 \text{ cm}^{-2}$ dislocations in the wing region and in the order of 10^{10} cm^{-2} dislocations in the GaN seed area [9]. Consequently, the ridge-waveguide laser diode stripes were placed in the low-dislocation-density area between the GaN seed and the center of the SiO_2 stripe region.

Figure 3(a) shows the voltage-current (V-I) and light output power-current (L-I) characteristics of a $2\mu\text{m} \times 300\mu\text{m}$ ridge-waveguide laser diode device operating under cw conditions at room temperature. As can be seen, cw threshold currents as low as 41 mA have been achieved at room temperature, which corresponds to a current density of 6.8 kA/cm^2 for this device. The operating voltage at threshold was 6.0 V. The maximum light output power was greater than 20 mW with a differential quantum efficiency of about 0.5 W/A. Figure 3(b) shows the cw light output vs. current characteristic for a laser diode measured at different heatsink temperatures. CW laser operation was possible up

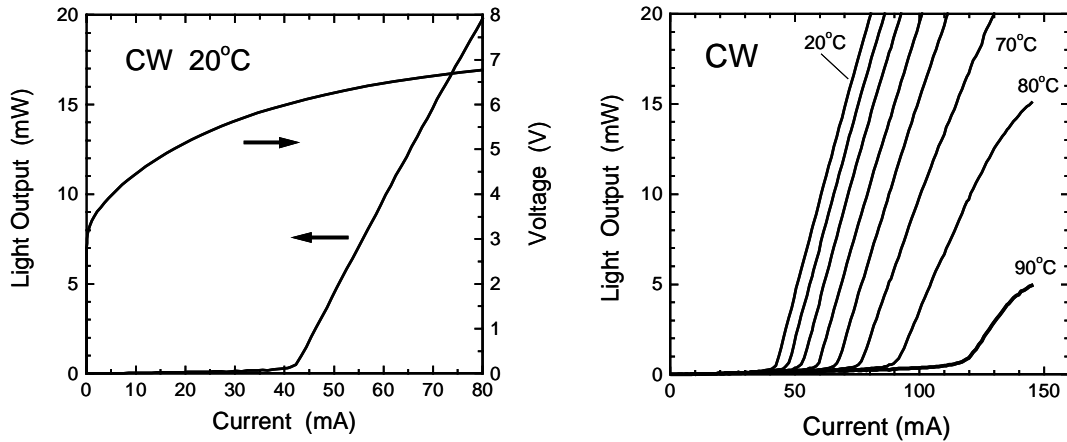


Figure 3: a) Current-voltage (V-I) and light output-current (L-I) characteristic for a 2 μm ridge waveguide laser diode under cw operation at 20°C. b) CW L-I characteristics for the same laser diode recorded for heatsink temperatures from 20°C to 90°C.

to a heatsink temperature of 90°C. The differential quantum efficiency remains almost unchanged up to 70°C. Note that, due to Joule heating during cw operation, the actual pn-junction temperature is higher than the heat sink temperature. From the increase in threshold current between low-duty-cycle-pulsed and cw operation, we estimate the actual device temperature to be about ~25°C higher than the heat-sink temperature. For the amount of dissipated electric power, this corresponds to a thermal resistance of about 35 K/W for p-side-up mounted lasers on ELOG on sapphire substrates. The temperature dependence of the cw threshold current yields a characteristic temperature T_0 of 81K in the vicinity of room temperature. Above 70°C the slope efficiency decreases rapidly and a super-exponential increase in threshold current can be observed, which we attribute to increased carrier spillover at these elevated temperatures. The room-temperature cw emission spectrum of the laser diode device measured at 10 mW light output is shown in Fig. 4. Multiple longitudinal modes can be clearly observed with the emission peak near 398 nm.

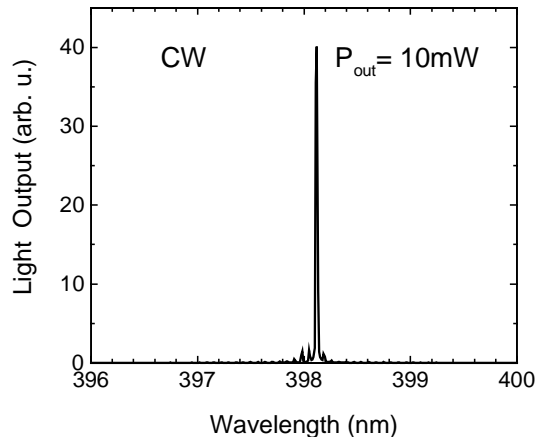


Figure 4: Room-temperature emission spectrum for a 300 μm ridge waveguide laser diode measured at 10 mW cw output power.

In order to characterize the internal quantum efficiency and distributed loss in the laser structures we measured the cw light output vs. current (L-I) characteristic of laser diodes for different cavity length as shown in Fig. 5(a). The inverse of the measured slope efficiency was then plotted vs. the cavity length of the laser diodes as shown in Fig. 5(b). For each cavity length we used a set of four samples in order to obtain a larger statistic for our fit. Using the following well-known relationship between differential quantum efficiency η_D , the internal quantum efficiency η_i , the distributed loss α , the cavity length L , and the front and back mirror reflectivity R_F and R_B ,

$$\frac{1}{\eta_D} = \frac{1}{\eta_i} \cdot \left(1 + \frac{2 * \alpha * L}{\ln\left(\frac{1}{R_F * R_B}\right)} \right),$$

we were able to describe the experimental results with parameters for the distributed loss of $\alpha = 40 \pm 4 \text{ cm}^{-1}$ and an internal quantum efficiency of $\eta_i = 32 \pm 5 \%$. We assumed a front mirror reflectivity of $R_F = 18\%$ and a backside mirror reflectivity of $R_B = 90\%$ for this least square fit. These values are very similar to those we obtained for laser diodes directly grown on sapphire substrates, although the distributed loss was somewhat higher ($\alpha = 48 \pm 6 \text{ cm}^{-1}$) in the later case. However both were still within the margin of error in our data.

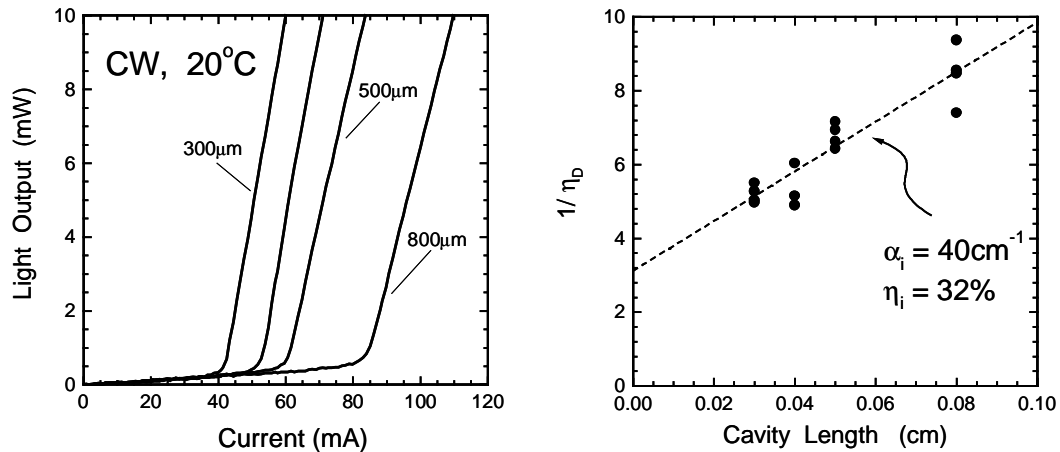


Figure 5: a) CW L-I characteristics for laser diodes on ELOG with cavity length of 300µm, 400µm, 500µm and 800µm. b) Inverse of the differential quantum efficiencies of the cw light output of a series of laser diodes ranging from 300µm to 800µm.

One major impediment to the development of high-performance III-V nitride laser diodes remains the efficient dissipation of heat generated from the active area of the device. The high thermal resistance of the sapphire substrate and the relatively high

current densities combine to degrade the device performance due to excessive heating during operation. Although thinning the sapphire substrate can reduce thermal resistance of the device, these approaches have limitations, e.g., how thin the sapphire substrate can be polished before the film starts to disintegrate. A comparison of thermal resistance values vs. the substrate thickness is shown in Fig. 6 for lasers on sapphire, lasers on ELOG on sapphire, and lasers with the sapphire substrate removed. The lines represent calculated curves based on a model published by Joyce and Dixon [15]. The device structure used in the calculation is basically the same as described earlier in the present paper. The only difference for the laser device on sapphire compared to that on ELOG on sapphire is the thickness of the GaN:Si buffer layer. For the ELOG device the thickness of this layer amounts to a total of 19 μm , whereas it is only 5 μm for the laser diode directly grown on sapphire. As can be seen from Fig. 6, increasing the thickness of the GaN film on sapphire actually improves the thermal resistance of the device, with the thermally highly conductive GaN buffer layer acting as a lateral heat spreader. This is also in good agreement with experimental data indicated by the symbols in Fig. 6. Nevertheless, a significant reduction in thermal resistance can be achieved by completely removing the sapphire substrate.

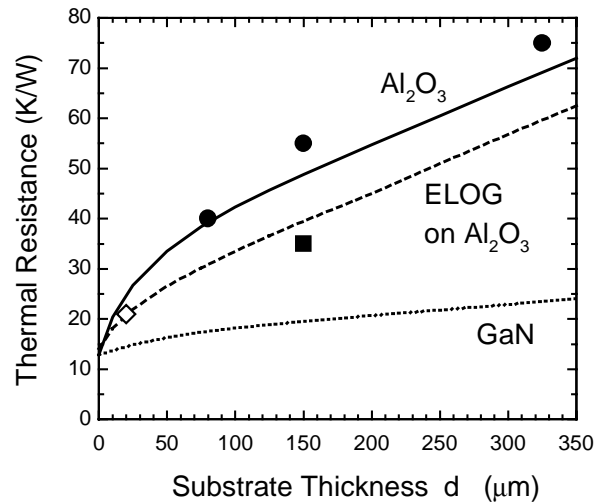


Figure 6: Thermal resistance for $2 \times 500 \mu\text{m}^2$ laser diodes vs the substrate thickness. The lines represent calculated curves for laser directly grown on sapphire (solid), on ELOG on sapphire (dashed), and lasers on GaN (dotted). The symbols represent measured data for lasers on sapphire (circles), lasers on ELOG (square) and lasers on Cu substrates (diamond).

In order to reduce the thermal resistance of laser diodes we have successfully separated and transferred laser diodes from sapphire onto Cu substrates. The separation of the LDs from sapphire was accomplished by using a laser lift-off (LLO) process in which a single XeCl excimer laser pulse was directed through the transparent sapphire substrate. The absorption of the 308 nm radiation by the GaN at the interface induces rapid thermal decomposition of the interfacial layer. Heating the structure above the

melting point of Ga completed the separation process. The free-standing InGaAlN laser diode membranes were then transferred and bonded at a temperature of $\sim 200^\circ\text{C}$ onto a Cu substrate by using the indium layer as a bond interface. Details of the lift-off and transfer process can be found in Refs. 16-19. Since the thermal conductivity of Cu ($R_{\text{th}} \sim 4 \text{ W/cm-K}$) is about 10 times larger than that of sapphire ($R_{\text{th}} \sim 0.4 \text{ W/cm-K}$), the thermal resistance of the laser diode can be greatly reduced. From the wavelength shift between pulsed and cw operation we estimate that the thermal resistance of our laser device on Cu is in the order of 21-27 K/W compared to 35-40 K/W for the same lasers on sapphire substrate. As a consequence of the reduced thermal resistance, laser devices on Cu could be driven at much higher dc current levels as shown in Fig. 7. As can be seen, we were able to operate laser diodes on copper substrates up to cw output power of more than 100mW, whereas the same laser devices on sapphire did not exceed 50mW.

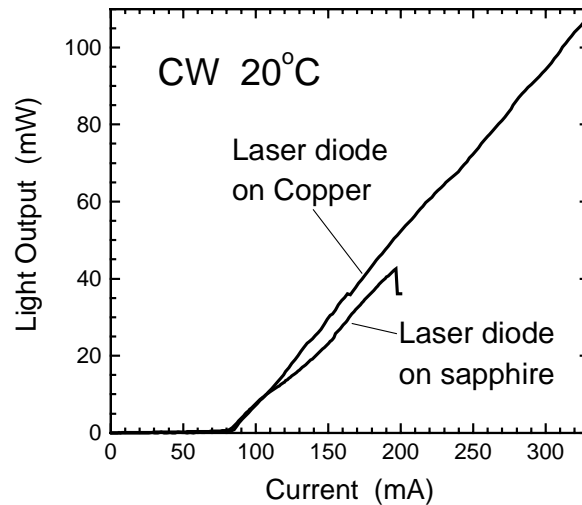


Figure 7: CW L-I characteristics for a $3\mu\text{m}$ ridge-waveguide laser diode on Cu substrate.

SUMMARY

In summary, we have demonstrated room-temperature cw operation of InGaN MQW laser diodes grown on low-dislocation-density substrates obtained by laterally epitaxially overgrown GaN on sapphire. The ridge-waveguide laser diodes exhibited cw threshold currents as low as 41 mA and threshold voltages of 6.0 V. We find only small differences in the internal quantum efficiency and distributed loss of laser diodes grown on sapphire compared to laser grown on ELOG, although we found the distributed loss to be higher in laser grown on sapphire. The thermal resistance was significantly reduced by transferring laser onto Cu, which resulted in an increased cw light output of more than 100mW.

REFERENCES

1. S. Nakamura, M. Senoh, S. Nagahama, N. Iwasa, T. Yamada, T. Matsushita, H. Kiyoku, and Y. Sugimoto, *Jpn. Jour. Applied Physics* **35**, pp. L74 – L76 (1996).
2. S. Nakamura, M. Senoh, S. Nagahama, N. Iwasa, T. Yamada, T. Matsushita, H. Kiyoku, and Y. Sugimoto, *Applied Physics Lett.* **72**, pp. 211-213 (1998).
3. S. Nakamura, M. Senoh, S. Nagahama, N. Iwasa, T. Yamada, T. Matsushita, H. Kiyoku, and Y. Sugimoto, *Applied Physics Lett.* **73**, pp. 832-834 (1998).
4. S. Nagahama, N. Iwasa, M. Senoh, T. Matsushita, Y. Sugimoto, H. Kiyoku, T. Kozaki, M. Sano, H. Matsumura, H. Umemoto, K. Chocho, T. Mukai, *Jpn. Jour. Applied Physics* **39**, pp. L647 (2000).
5. See for example article in *The Nikkei Industrial Daily Tuesday Edition*, January 12th, 1999.
6. T. Kobayashi, F. Nakamura, K. Naganuma, T. Tojyo, H. Nakajima, T. Asatsuma, H. Kawai, and M. Ikeda, *Electronics Lett.* **34** (15), 1494 (1998).
7. A. Kuramata, S. Kubota, R. Soejima, K. Domen, K. Horino and T. Tanahashi, *Jpn. J. Appl. Phys.* **37**, L1373 (1998).
8. M. Kuramoto, C. Sasaoka, Y. Hisanaga, A. Kimura, A.A. Yamaguchi, H. Sunakawa, N. Kureda, M. Nido, A. Usui and M. Mizuta, *Jpn. J. Appl. Phys.* **38**, L184, (1999).
9. M. Kneissl, D.P. Bour, C.G. Van de Walle, L.T. Romano, J.E. Northrup, R.M. Wood, M. Teepe, N.M. Johnson, *Applied Physics Lett.* **75**, 581 (1999).
10. A. Sakai, H. Sunakawa, A. Usui, *Applied Physics Lett.* **71**, 2259 (1997).
11. T.S. Zheleva, O. Nam, M.D. Bremser, R.F. Davis, *Applied Physics Lett.* **71**, 2472 (1997).
12. H. Miyake; A. Motogaito; K. Hiramatsu, *Jpn. J. Appl. Phys.* **38**, L1000 (1999).
13. C. Youtsey, I Adesida, G. Bulman, *Applied Physics Lett.* **71**, 2151 (1997).
14. C. Youtsey, L.T. Romano, R.J. Molnar, I. Adesida, *Applied Physics Lett.* **74**, 3537 (1999).
15. W.B. Joyce and R.W. Dixon, *Journal of Appl. Phys.* **46**, 855 (1975).
16. W.S. Wong, N.W. Cheung, T. Sands, *Appl. Phys. Lett.* **72**, 599 (1998).
17. W.S. Wong, M. Kneissl, P. Mei, D.W. Treat, M. Teepe and N.M. Johnson, *Jpn. J. Appl. Phys.* **39**, L1203 (2000)
18. W.S. Wong, M. Kneissl, P. Mei, D.W. Treat, M. Teepe, and N.M. Johnson, submitted for publication in *Appl. Phys. Lett.* .
19. M. Kneissl, W.S. Wong, D.W. Treat, M. Teepe, N. Myashita, N.M. Johnson, submitted for publication in *IEEE Journal of Selected Topics in Quantum Electronics*.